A Model of the Cellular Iron Homeostasis Network Using Semi-Formal Methods for Parameter Space Exploration

Nicolas Mobilia
UJF-Grenoble 1 / CNRS
TIMC-IMAG UMR 5525,
Grenoble, F-38041, France
nicolas.mobilia@imag.fr

Alexandre Donzé
EECS Department
University of California Berkeley
Berkeley, CA 94720 USA
donze@eecs.berkeley.com

Jean Marc Moulis
UJF-Grenoble 1 / CNRS UMR 4952,
Institut de Recherches en Technologies et Sciences pour le Vivant,
17 rue des Martyrs,
38054 Grenoble
jean-marc.moulis@cea.fr

Éric Fanchon
UJF-Grenoble 1 / CNRS
TIMC-IMAG UMR 5525,
Grenoble, F-38041, France
eric.fanchon@imag.fr

This paper presents a novel framework for the modeling of biological networks. It makes use of recent tools analyzing the robust satisfaction of properties of (hybrid) dynamical systems. The main challenge of this approach as applied to biological systems is to get access to the relevant parameter sets despite gaps in the available knowledge. An initial estimate of useful parameters was sought by formalizing the known behavior of the biological network in the STL logic using the tool Breach. Then, once a set of parameter values consistent with known biological properties was found, we tried to locally expand it into the largest possible valid region. We applied this methodology in an effort to model and better understand the complex network regulating iron homeostasis in mammalian cells. This system plays an important role in many biological functions, including erythropoiesis, resistance against infections, and proliferation of cancer cells.

1 Introduction

In cellular biology, the value of the parameters are uncertain (when a measurement does exist) or not known at all (unmeasured or not computable from first principles). It is well known that values of kinetic constants obtained from in vitro measurements on purified enzymes can be significantly different from the in vivo values, due to interactions with other cell components, to regulatory modifications of enzymes, to sequestration, to anomalous diffusion or still other phenomena. In addition, the values available from the literature are heterogeneous (measurement performed in different species, or on different cell types, or in different conditions). Two sets of measurements performed on identical cell types placed in supposedly identical conditions can also be qualitatively different for multiple reasons (undetected heterogeneity of cell populations, different batches of antibodies used for detection, for instance). The fact that the available data and pieces of information are generally too scarce with respect to the size of dynamical cell models forces the modeler to include every bit of available data, at the cost of increased heterogeneity and thus increased uncertainty. But even with such an inclusive strategy the amount of data remains inadequate to identify a fully instantiated model.

The complexities and heterogeneity of both the parameter values and the analytical expressions of the terms entering the differential equations describing a biological system implies such a system results from a family of dynamical systems, instead of a single one. The properties which formalize experimentally observed behaviors should thus be robust with respect to the uncertainties mentioned above.

Ezio Bartocci and Luca Bortolussi (Eds.): HSB 2012
EPTCS 92, 2012, pp. 42–57, doi:10.4204/EPTCS.92.4

These issues are considered in the present paper and the semi-formal method implemented to explore the parameter space is applied to an important question in biology: how iron homeostasis is maintained in mammalian cells? Iron is the most abundant transition metal required by most forms of life. The largest part needed by animals ends up in red blood cells, but all cell types do use the metal [2]. Iron is handled by specific molecules in animal physiology, so as to avoid the deleterious reactions the iron ions catalyze, conversion of oxygen derivatives into reactive species (the reactive oxygen species, ROS) prominent among them [15]. The mandatory requirement for iron and the negative impact the metal may have on cellular function call for a tight regulation of its use [7]. Deregulation translates into cellular oxidative damage: this links iron homeostasis to the redox balance in animal, and other, cells. These connections underlie scores of (human) pathological situations in which these homeostatic systems (iron and redox homeostasis) are perturbed.

Our approach rests on the following points: we deal explicitly with the parameter space, and we do not focus on a single instantiation of the model parameters. When the parameter values are uncertain due to the fact that they have been measured in different cell types or in different conditions, the data are formally represented by inequalities. In other words, we do not assign the measured value directly to the parameter but rather impose inequality constraints on that parameter. If there is no measurement at all, bounds are chosen to define a physiologically reasonable domain. Observed behavioral properties can be formalized using a temporal logic formalism. Then the behaviors of the parametrized system are explored by sampling predefined volumes of parameter space (including initial conditions and model parameters), and the instantiated models that satisfy the temporal logic formula are identified. As illustrated below this very basic scheme needs some elaboration to be applied to the modeling of a complex, yet simplified, biological phenomenon.

The biological network we have built for iron homeostasis is presented in section 2. The system of differential equations is introduced in section 3 and its dynamical properties explored in the following section.

2 Biological network

We are considering regulation of iron handling in cell types which acquire iron by endocytosis of the transferrin-transferrin receptor complex (most of them) and express an iron exporter in the form of ferroportin. Proper supply of iron to animal cells is required to avoid deleterious effects of too much or too little iron as such imbalance jeopardizes the proper function of cells and may lead to death. Regulation of iron supply occurs at two levels, a systemic one and a local one organized around Iron Regulatory Proteins. The latter are the main focus of this study since they directly act on the molecular nodes of the considered network.

2.1 Species

The considered network is shown in Figure 1 A. It contains five species: Iron Regulatory Protein (IRP, no difference is made between the two known proteins displaying this function), iron (Fe), ferritin (Ft), the transferrin receptor (TfR1) and ferroportin (FPN1a). Moreover, transferrin (Tf) is a protein which carries iron in the blood stream throughout the body, and which can bind zero, one, or two iron atoms. It is the main provider of iron to most cells and, as such, it is an input of the network. The circle labeled by Fe_out is the iron exported out of the cell. The circle labeled by Fe_cons represents the iron consumed for the cell needs.

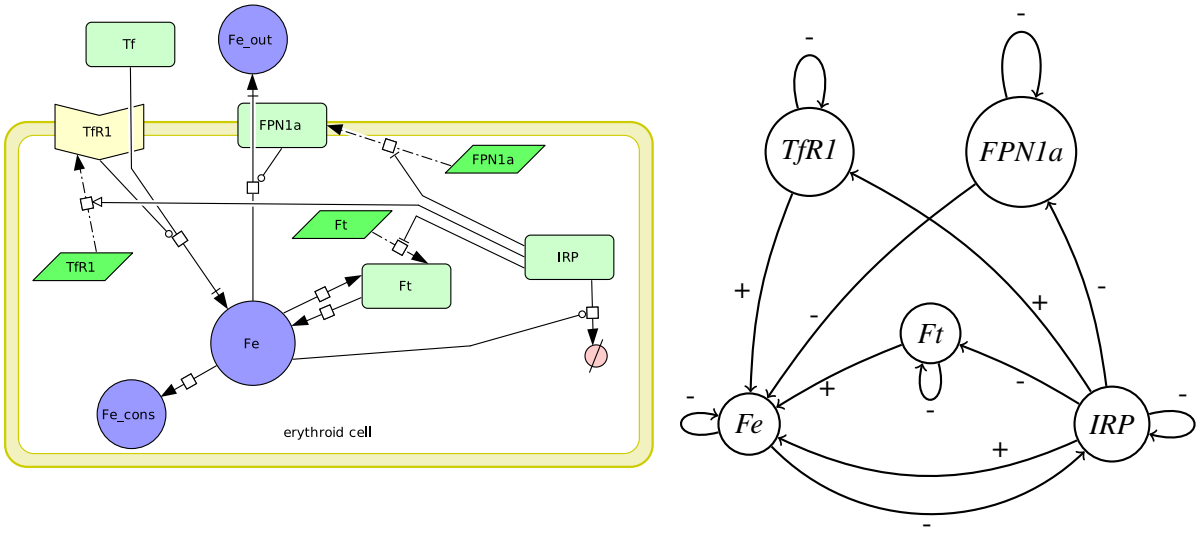

A) B)

Figure 1: A) Schematic representation of the main biological processes involved in the cellular homeostatic control of iron.
The dashed arrows represent translation of mRNA into proteins. The arrow ending in an unfilled white arrow represents amplification of translation, while the lines with a broken ending arrowhead represent inhibition of translation. The lines ending with a combined perpendicular stroke and arrow represent iron transport through membranes. The arrow leading to a pink circle indicates degradation. Finally, the two regular arrows represent the loading/unloading of iron into/from the ferritins and the consumption of iron for the cell needs. The green rounded rectangles represent proteins, the green parallelograms represent mRNA, and the blue circles represent atoms. The yellow concave hexagon represents the transferrin receptor. This diagram was drawn with the software CellDesigner [14].
B) Interaction graph defined by the equations. The signs on the arrows indicate whether the interaction is positive or negative.

The IRP are proteins which can bind to a specific hairpin-like structure on mRNA, called Iron Responsive Element (IRE). Depending on the position of the IRE on the non-coding sequence of mRNA, two main outputs may result:

- If the IRE is located at the beginning of the mRNA, in the 5' untranslated region (UTR), the binding of the IRP prevents the translation machinery from binding to the mRNA and translating it, so the binding of the IRP leads to a reduced quantity of the corresponding protein;
- If the IRE is located at the end of the mRNA (3'-UTR), the binding of the IRP inhibits the degradation of this mRNA, leading to an increase in the quantity of translated protein.

In the presence of enough iron, the regulatory activity of the IRP is decreased by different molecular mechanisms [24].

The iron species (Fe) represents the cellular iron which is available for cellular processes. The actual form of this iron in biological cells is still a topic of discussion. A virtual species, which we call "Fe", is introduced in order to model the usable iron in the cell. If this amount of intracellular iron becomes too low, the cell cannot maintain vital functions and dies.

Ferritin is a protein which stores iron [3]. The complex mechanisms of iron loading into and release from ferritin are not considered here. The mRNA of both ferritin subunits contain an IRE on their 5'-UTR regions, and the IRP inhibit their translation.

Transferrin receptors are located on the surface of the cell [1]. The fixation of transferrin on its receptor leads to the endocytosis of the complex. This process involves several steps and releases iron into the cell. Transferrin receptor mRNA contain five IRE in the 3'-UTR region, which is stabilized upon IRP binding. The density of transferrin receptor at the cell surface is thus correlated with the IRP activity.

Finally, ferroportin (FPN1a) is an iron exporter located at the surface of some cells [20]. A form of FPN1a contains an IRE on its 5'-UTR mRNA region, so the translation is inhibited by the presence of IRP.

2.2 Behavior

A qualitative description of the system has been obtained through a large body of biological experiments and we selectively summarize them here.

If the amount of iron is sufficient (*iron-replete* situation), the cell is in a stationary state. Assuming that the iron provision stays constant, the concentration of each protein described in Figure 1 A does not vary. In this state, the IRP activity is expected to be relatively low. In the case of too much iron (which is not studied here), the saturation level of transferrin increases, the IRP activity reaches a minimum and inhibits translation of the iron importer (TfR1) to minimize cellular iron input.

From the iron-replete stationary state, if the cells become *iron-depleted*, the inhibition of IRP activity by iron decreases. Thus, the increasing IRP activity leads to an increase in the transferrin receptor concentration and to a decrease in ferroportin concentration. This, in turn, leads to an augmentation in the amount of iron entering the cell and a reduction in the amount of iron leaving the cell. Moreover, the iron loaded in ferritin is released to convert stored iron into a form available for biosynthetic purposes. This release allows the cell to face a temporary reduction in the level of iron (typically because of a reduction in the iron input) for a certain amount of time. When ferritin is depleted, and if there is still no iron input mediated by the receptor TfR1, the cell runs out of iron and enters in a cellular death process. The IRP regulating system is effective as long as the iron level remains low. When the iron level regains an acceptable level again, the IRP activity decreases, and the amount of filled ferritin goes up, regenerating the stock of stored iron.

3 ODE modeling

In this section we describe the differential equations that we derived to specifically describe the evolution of the concentration of each species over time. Some processes in the iron homeostasis network are in fact a composition of many reactions, and the choice of an analytical expression to represent them is not straightforward. This is the case of the iron entry mediated by TfR1, which involves endocytosis, and of the loading of iron in ferritin, for example.

3.1 Iron equation

In the cell, when the level of iron becomes low, some iron-proteins release their iron content, by protein degradation for instance, which contributes to refill the iron pool; however, only iron release from ferritin is considered in our model without affecting the general validity of the reasoning. The equation defining

the iron concentration is:

$$\frac{\mathrm{d}Fe}{\mathrm{d}t} = k_{Fe\_input} \cdot TfR1 \cdot Tf_{sat} - n_{Ft} \cdot \frac{\mathrm{d}Ft}{\mathrm{d}t} - k_{Fe\_export} \cdot Fe \cdot FPN1a - k_{Fe\_cons} \cdot Fe \tag{1}$$

The import of iron into the cell is proportional to the concentration of transferrin receptor and to the average amount of iron bound to transferrin (called transferrin saturation): Tf_{sat}. The second term describes the storage or release of iron due to the synthesis or degradation of ferritin. This variation is equal to the number of iron atoms per ferritin molecule (aka n_{Ft}) times the variation in the ferritin concentration (we consider that (i) iron release occurs only when ferritin is degraded (ii) synthesized ferritins are very quicky filled with iron). The third term describes the export of iron out of the cell as proportional to the iron and FPN1a concentration. The export parameter is k_{Fe_export}. Finally, within the cell, iron is used for many purposes; this consumption of iron is represented by the last term in our equation ($k_{Fe\_cons} \cdot Fe$). For the sake of simplicity, we consider this consumption term (which represents a whole set of cellular processes) to be proportional to the iron concentration. The export of iron by FPN1 forms that are not regulated by IRP can be accounted for by this term.

3.2 IRP equation

The equation describing the IRP concentration is:

$$\frac{\mathrm{d}IRP}{\mathrm{d}t} = k_{IRP\_prod} - k_{Fe\to IRP} \cdot sig^{+}(Fe, \theta_{Fe\to IRP}) \cdot IRP - k_{IRP\_deg} \cdot IRP \tag{2}$$

We define a constant rate of production of IRP by k_{IRP_prod}. The concentration of iron regulates the activity of IRP. The degradation of IRP is described by a constant basal term ($k_{IRP\_deg} \cdot IRP$) and an iron-related term ($k_{Fe\to IRP} \cdot sig^{+}(Fe, \theta_{Fe\to IRP}) \cdot IRP$). Then, if the iron level is significantly below the threshold $\theta_{Fe\to IRP}$, the degradation rate is $k_{IRP\_deg} \cdot IRP$. If the iron concentration is significantly above this threshold, the degradation rate is $(k_{Fe\to IRP} + k_{IRP\_deg}) \cdot IRP$, where $k_{Fe\to IRP}$ is the parameter describing the inhibition of IRP by iron.

The sigmoid function is defined such that:

$$sig^{+}(x, \theta) = \frac{x^n}{x^n + \theta^n}$$

where x is a concentration variable, θ is the threshold and n defines the steepness of the sigmoid. In our model, we use $n = 30$, which corresponds to a very steep sigmoid.

3.3 Ferritin equation

To model the temporal evolution of ferritin, we assume that each ferritin protein is rapidly filled with iron atoms, right after its synthesis is completed. In other words the amount of empty ferritin is negligible. The variable Ft thus represents the concentration of filled ferritin proteins within the cell. The equation describing the evolution of the concentration of ferritin is:

$$\frac{\mathrm{d}Ft}{\mathrm{d}t} = k_{Ft\_prod} - k_{IRP\to Ft} \cdot sig^{+}(IRP, \theta_{IRP\to Ft}) - k_{Ft\_deg} \cdot Ft \tag{3}$$

We consider a basal production rate described by k_{Ft_prod}. The second term describes the regulation by IRP. We use a sigmoidal regulation here, but we could consider other dynamics. If the activity of IRP is above the threshold $\theta_{IRP\to Ft}$, the production rate is lowered by $k_{IRP\to Ft}$. It follows that $k_{IRP\to Ft}$ has to be lower or equal to k_{Ft_prod}: as IRP inhibits translation, this inhibition should never lead to a negative production rate. Finally, the third term ($k_{Ft\_deg} \cdot Ft$) describes the spontaneous degradation of ferritin.

3.4 Ferroportin equation

The equation describing the ferroportin concentration is very similar to that of ferritin. The equation is:

$$\frac{\mathrm{d}FPN1a}{\mathrm{d}t} = k_{FPN1a\_prod} - k_{IRP\to FPN1a} \cdot sig^{+}(IRP, \theta_{IRP\to FPN1a}) - k_{FPN1a\_deg} \cdot FPN1a \tag{4}$$

The first term describes the basal production of FPN1a. The second term expresses the regulation of IRP on the translation of FPN1a. With the same reasoning as previously, the regulation parameter $k_{IRP\to FPN1a}$ has to be lower or equal to the production parameter k_{FPN1a_prod}. The dynamics of IRP regulation on Ft and FPN1a are considered similar because both FPN1a and Ft mRNAs have a single IRE located in the 5'-UTR region without experimental evidence of major differences between the two.

3.5 Transferrin receptor equation

The concentration of the transferrin receptor evolves according to the following equation:

$$\frac{\mathrm{d}TfR1}{\mathrm{d}t} = k_{TfR1\_prod} + k_{IRP\to TfR1} \cdot IRP - k_{TfR1\_deg} \cdot TfR1 \tag{5}$$

The production of TfR1 includes a basal rate k_{TfR1_prod} and it is increased proportionally to the IRP concentration. This is taken into account in the term $k_{IRP\to TfR1} \cdot IRP$. This term is different from those describing the regulation of ferritin and ferroportin in an effort to consider the binding of several IRPs to a single TfR mRNA molecule (since it contains several IREs). The half-life of TfR1 mRNA is considered proportional to the IRP concentration, although this is a rough approximation [13]. The last term of the equation represents the spontaneous degradation.

3.6 Interaction graph

The interaction graph is a useful tool to visualize the pattern of interactions in a system of differential equations. It is defined from the Jacobian matrix of the system. Each non-zero element in this matrix indicates that a species influences another species. The nodes of the interaction graph are the dynamical variables of the system (concentration of biological species), and each arc represents the influence of a node on another, i.e. a non-zero element of the Jacobian matrix. The sign of this element determines whether the influence is positive or negative. Of course it is possible that the sign of the elements depends on the point of phase space at which the Jacobian is evaluated, but in our model the signs are constant. The interaction graph we obtain is shown in Figure 1 B.

We define a negative (resp. positive) circuit (closed path) as a succession of arrows in the interaction graph such that the product of the signs labelling these arrows is negative (resp. positive). This graph contains three negative circuits of length greater than one (IRP→Fe→IRP ; IRP→FPN1a→Fe→IRP and IRP→TfR1→Fe→IRP), and five negative loops corresponding to spontaneous degradation or consumption. It also contains one positive circuit (IRP→Ft→Fe→IRP). The presence of these circuits, together with the presence of non-linear terms in the equations, generate a complex dynamical behavior.

4 Methodology

In this section we present our strategy to study the system. We first translate all available biological data into inequalities on parameters and variables. Then, we formally define the expected behavior for the two modes described in Section 2.2: the *iron-replete* mode and the *iron-depleted* mode. Finally we look for a subspace which robustly verifies this behavior.

4.1 Parameter search space

The parameter space of the system is twenty-dimensional. To define an initial parameter search space, we combined published data from different sources as shown in table 1. Whenever possible, the available data obtained with erythroleukemic cells have been used, as these cells are relatively immature and proliferate, as considered for the initial steady state.

In mouse macrophages, half-life of FPN1a seems to be more than 20 hours [18]	$0 < k_{FPN1a\_deg} \leq 9.6 \times 10^{-6}\ s^{-1}$
The production rate of TfR1 was estimated at 7×10^{-6} pg/cell/min as in [22]	$1.0 \times 10^{-13} \leq k_{TfR1\_prod} \leq 2.0 \times 10^{-13}$ mol/L/s
The half-life of IRP is 12-15 hours in H1299 human lung cancer cells [11]	$1.28 \times 10^{-5} \leq k_{IRP\_deg} \leq 1.6 \times 10^{-5}\ \mathrm{s}^{-1}$
In human erythroleukemia cell line K562, half-life of TfR1 is 8 hours [25]	$2.0 \times 10^{-5} \leq k_{TfR1\_deg} \leq 3.0 \times 10^{-5}\ \mathrm{s}^{-1}$
The TfR1 production rate enhanced by IRP is 6×10^{-5} pg/cell/min [22]	$4.2 \times 10^{-5} \leq k_{IRP \to TfR1} \leq 14.4 \times 10^{-5}\ \mathrm{s}^{-1}$
In human erythroleukemia cell line K562, iron input is up to $7.2 \pm 2.4 \times 10^4$ Fe atoms/cell/min [23]	$2 \times 10^{-2} \leq k_{Fe\_input} \leq 3.9 \times 10^{-2}\ \mathrm{s}^{-1}$
In mammalian cells, the number of iron atoms in ferritin up to 4500 [3]	$0 < n_{Ft} \leq 4500$
Human normal saturation level of transferrin is within 25% and 45% [21], we take 30%	$Tf_{sat} = 0,3$ (in iron-replete situation)
In human erythroid cells, a fraction of the iron exporter (FPN1) is not IRP-regulated [6]. The amount of iron needed for biosynthesis ("consumed") is higher than the exported one.	$k_{Fe\_cons} \geq k_{Fe\_export} \cdot FPN1a$ (in iron-replete situation)
A higher limit for the iron pool in erythroleukemic cells is set at 2 μmol/L [12]	$Fe \leq 2 \times 10^{-6}$ mol/L
In rats liver, the IRP concentration in around 0.11 pmol/mg of cytosolic protein under normal conditions [4]	$3 \times 10^{-9} \leq IRP \leq 10.7 \times 10^{-9}$ mol/L (in iron-replete situation)
In human erythroleukemic (K562) cells, there are 140,000 transferrin receptors by cell [17]	$1.0 \times 10^{-8} \leq TfR1 \leq 10.0 \times 10^{-8}$ mol/L (in iron-replete situation)

Table 1: The left column shows the data collected in the literature; the right column describes the corresponding interval on parameters and variables, and the inequalities deduced.

We then obtained intervals for eight parameters, including one in the iron-replete situation. Moreover, we derived an inequality linking k_{Fe_cons}, k_{Fe_export} and $FPN1a$. Finally, we found data on the value of three variables (Fe, IRP and $TfR1$) among which two are related to the iron-replete situation.

In order to evaluate the search space for the twelve other parameters, we proceeded by analogy. For example, we had no information on the basal production rate of ferritin, ferroportin and IRP, but we knew an interval for the production rate of the transferrin receptor. We then assumed that the basal production rate of ferroportin was neither more than 1000 times higher than the highest possible transferrin

receptor basal production rate, nor 1000 times lower than the lowest. Concerning the thresholds parameters, we simply assumed that their possible intervals were the same as for the corresponding protein concentrations.

4.2 The iron-replete steady state

The iron-replete situation is modeled by a steady state, so we do not consider evolutions of the variables over time. In this state, the value of the variable representing the iron concentration is expected to be significantly higher than the threshold $\theta_{Fe\to IRP}$. We can thus infer that the sigmoidal term $sig^+(Fe,\theta_{Fe\to IRP})$ is very close to one, and we replace it. The value of the variable representing the IRP activity is also expected to be largely below the thresholds $\theta_{IRP\to Ft}$ and $\theta_{IRP\to FPN1a}$. We then consider that the two sigmoidal functions $sig^+(IRP,\theta_{IRP\to Ft})$ and $sig^+(IRP,\theta_{IRP\to FPN1a})$ are very close to zero. These simplifications contribute to reducing the complexity of the system. Note that this amounts to approximating the sigmoid by step functions, and consequently the system could be viewed as an hybrid system.

We developed two complementary approaches for studying the system in the iron-replete steady state. The first consists in a mathematical analysis of the system. The second consists in performing deductions from the quantitative data.

Looking for a steady state, we set the derivatives in the model to zero and solved the resulting algebraic system using the symbolic solver Maxima [19]. This way, we could prove the existence of one unique stationary point, given by Equations (6) to (10).

$$Fe = \frac{Tf_{sat}\cdot k_{FPN1a\_deg}\cdot k_{Fe\_input}\cdot\left(k_{TfR1\_prod}\cdot\left(k_{IRP\_deg}+k_{Fe\to IRP}\right)+k_{IRP\to TfR1}\cdot k_{IRP\_prod}\right)}{\left(k_{Fe\_export}\cdot k_{FPN1a\_prod}+k_{Fe\_cons}\cdot k_{FPN1a\_deg}\right)\cdot\left(k_{IRP\_deg}+k_{Fe\to IRP}\right)\cdot k_{TfR1\_deg}} \tag{6}$$

$$Ft = \frac{k_{Ft\_prod}}{k_{Ft\_deg}} \tag{7}$$

$$FPN1a = \frac{k_{FPN1a\_prod}}{k_{FPN1a\_deg}} \tag{8}$$

$$IRP = \frac{k_{IRP\_prod}}{k_{IRP\_deg}+k_{Fe\to IRP}} \tag{9}$$

$$TfR1 = \frac{\left(k_{IRP\_deg}+k_{Fe\to IRP}\right)\cdot k_{TfR1\_prod}+k_{IRP\to TfR1}\cdot k_{IRP\_prod}}{\left(k_{IRP\_deg}+k_{Fe\to IRP}\right)\cdot k_{TfR1\_deg}} \tag{10}$$

We then considered the stability of this stationary point by computing its Jacobian matrix since an unstable stationary point cannot obviously represent an observed cellular state. The obtained Jacobian matrix is shown in equation (11).

$$\begin{pmatrix} -FPN1a\cdot k_{Fe\_export}-k_{Fe\_cons} & Tf_{sat}\cdot k_{Fe\_input} & -Fe\cdot k_{Fe\_export} & k_{Ft\_deg}\cdot n_{Ft} & 0 \\ 0 & -k_{TfR1\_deg} & 0 & 0 & k_{IRP\to TfR1} \\ 0 & 0 & -k_{FPN1a\_deg} & 0 & 0 \\ 0 & 0 & 0 & -k_{Ft\_deg} & 0 \\ 0 & 0 & 0 & 0 & -k_{IRP\_deg}-k_{Fe\to IRP} \end{pmatrix} \tag{11}$$

As this matrix is upper triangular, its eigenvalues are equal to its diagonal elements. It follows that all eigenvalues are real and negative, which proves the stability of the stationary point.

Another way to study the steady state consists in using the specific data we have on the variables at the stationary state and propagate them on the parameter space. For this purpose, we use Realpaver [16], an interval solver. The solver uses the algebraic equations between parameters and variables, as well as defined intervals and constraints, as inputs for the calculation. The aim of Realpaver is to reduce the provided intervals and consequently reduce the parameter space. The results are the following:

- $k_{FPN1a\_deg} \geq 1.0 \times 10^{-13}$ s^{-1} (initial interval: $[0.0,\ 9.6 \times 10^{-6}]$)
- $k_{FPN1a\_prod} \leq 9.6 \times 10^{-11}$ mol/L/s (initial interval: $[1.0 \times 10^{-18},\ 1.0 \times 10^{-10}]$)
- $k_{IRP\_prod} \geq 3.84 \times 10^{-14}$ mol/L/s (initial interval: $[1.0 \times 10^{-18},\ 1.0 \times 10^{-10}]$)
- $k_{Fe\_cons} \leq 3.39 \times 10^{-4}$ s^{-1} (initial interval: $[0.0,\ 1.0]$)
- $k_{Fe \to IRP} \leq 3.33 \times 10^{-2}$ s^{-1} (initial interval: $[1.0 \times 10^{-9},\ 1.0]$)

Realpaver returns intervals which are reduced by many orders of magnitude for four of the parameters. These results prove that some subspaces of the parameter space do not contain valid parameter sets, and then, need not be considered when searching for an parameter set producing an adequate iron-replete steady state. This will reduce the search of the parameter space in the next step (analysis of the dynamical behavior).

Besides, Realpaver makes no difference between variables and parameters considered in the algebraic system, they are all variables (unknowns). Consequently it also propagates the constraints from the parameters to the variables, and provides deductions on three variables in the iron-replete situation:

- $FPN1a \geq 1.04 \times 10^{-13}$ mol/L (initial interval: $[1.0 \times 10^{-13},\ 1.0 \times 10^{-5}]$)
- $Fe \geq 3.5 \times 10^{-8}$ mol/L (initial interval: $[0.0,\ 2.0 \times 10^{-6}]$)
- $TfR1 \leq 8.7 \times 10^{-8}$ mol/L (initial interval: $[1.0 \times 10^{-8},\ 1.0 \times 10^{-7}]$)

These results, provided by Realpaver in less than one second on a Core 2 Duo 3 GHz with 8 Gb of RAM, can be considered as deductions made from the initial data. Indeed, the difficulty in finding a valid parameter set is that steady state values must be within their intervals. These two approaches facilitate the manual search of an initial parameter space. The analytical solution of the equations indicates, for each parameter, the variables impacted by a change in the parameter value. We use this information to define an order for checking variables, such that there are parameters allowing us to adjust a variable value but not changing the value of the already correct variables. Consequently, to find an initial valid parameter set, one has only to tune some parameters to fix the value of the first variable, then tune some other parameters to fix the value of the second variable, and so on. If the value of one variable cannot be set in its interval, one has to step back and change the value of parameters used to fix the value of the previous variable. The variable order we use is: IRP, TfR1 (through the adjustment of $k_{IRP \to TfR1}$, k_{TfR1_prod} and k_{TfR1_deg}), FPN1a, Fe (through k_{Fe_cons}, k_{Fe_export} and k_{Fe_input}) and finally Ft. Using this method, we found the following initial parameter set, denoted as $\mathscr{P}_0$:

k_{TfR1_prod}	=	1.7×10^{-13}	mol/L/s	k_{FPN1a_deg}	=	5.0×10^{-6}	s^{-1}
k_{TfR1_deg}	=	2.4×10^{-5}	s^{-1}	k_{Fe_input}	=	3.0×10^{-2}	s^{-1}
n_{Ft}	=	400	-	k_{Ft_prod}	=	7×10^{-11}	mol/L/s
k_{IRP_prod}	=	8.0×10^{-12}	mol/L/s	k_{Ft_deg}	=	5.0×10^{-3}	s^{-1}
k_{Fe_export}	=	300	L/mol/s	$k_{Fe \to IRP}$	=	1.0×10^{-3}	s^{-1}
$\theta_{IRP \to FPN1a}$	=	3.0×10^{-8}	mol/L	$\theta_{Fe \to IRP}$	=	1.5×10^{-7}	mol/L
$k_{IRP \to FPN1a}$	=	5.0×10^{-13}	mol/L/s	k_{IRP_deg}	=	1.4×10^{-5}	s^{-1}
$k_{IRP \to TfR1}$	=	1.4×10^{-4}	s^{-1}	k_{FPN1a_prod}	=	2.5×10^{-12}	mol/L/s
k_{Fe_cons}	=	3.0×10^{-4}	s^{-1}	$\theta_{IRP \to Ft}$	=	3.0×10^{-8}	mol/L
$k_{IRP \to Ft}$	=	7×10^{-11}	mol/L/s				

It will be used as the initial parameter set for the exploration of the parameter space, as explained in the following section.

4.3 Dynamics in iron-depleted situation

We are now interested in the behavior of the network when the input of iron is cut. As a consequence, we need to compute the evolution of the system over time. For that, we use Breach [8, 9], a tool based on Matlab/C++. This tool allows not only to simulate differential systems, but also to express temporal logic formula and to check whether a trajectory satisfies or not a given formula.

We introduce briefly STL (Signal Temporal Logic). A more complete description can be found in [9]. Initially created for verifying the correctness of reactive programs, temporal logics provide languages to express properties over time-dependent phenomena for any kind of dynamical system. STL and its quantitative semantics [10] specializes into systems with continuous time and with real-valued states. An STL formula has the following syntax:

$$\varphi = \mu \ \texttt{|} \ (\varphi_1) \ \texttt{and} \ (\varphi_2) \ \texttt{|} \ \texttt{ev\_[a,b]} \ (\varphi) \ \texttt{|} \ \texttt{alw\_[a,b]} \ (\varphi) \tag{12}$$

where μ is an inequality constraint between expressions involving variables (written `var[t]`), constants or derivatives of a variable over time (written `ddt{var}[t]`). A formula is evaluated at each requested time (thereafter called "the current time"). A formula with a `and` statement is true if both φ_1 and φ_2 are true at the current time. The `ev_[a,b]` statement is true if φ holds at least once between the current time plus `a` and the current time plus `b`. If the interval is omitted, then `a` is 0 and `b` is inf, that is, the formula is true if φ holds at least once, anytime after the current time. The statement `alw_[a,b]` is true if φ holds between current time plus `a` and current time plus `b`. Again, if the interval is omitted then `a` is 0 and `b` is inf meaning in that case that the formula must hold all the time.

The experiment we want to simulate is the cut-off of iron entry for cells initially in the iron-replete situation. The total duration of the simulation is 48 hours, as the qualitative description of the iron-depleted situation tells us that significant changes can be seen in 24 hours. First we want the simulations to stabilize in a steady state corresponding to the iron-replete situation. Then, at time t=6 hours, we cut the entry of iron by setting Tf_{sat} to zero. We expect the system to turn on the IRP regulatory system in order to maintain a correct iron level for at least ten hours. To identify parameter values for which the simulations satisfy all theses properties, we use temporal logic formula.

We first want the system to be in a steady state corresponding to the iron-replete situation. To avoid an inappropriately long stabilization phase, we specify initial conditions close to the value of the stationary state. To ensure that the system reaches a steady state, we use the following temporal logic formula:

$$\begin{aligned}
\varphi_{S1} &= \texttt{abs(ddt\{Fe\}[t] / Fe[t]) < 1.0e-4} \\
\varphi_{S2} &= \texttt{abs(ddt\{Ft\}[t] / Ft[t]) < 1.0e-4} \\
\varphi_{S3} &= \texttt{abs(ddt\{FPN1a\}[t] / FPN1a[t]) < 1.0e-4} \\
\varphi_{S4} &= \texttt{abs(ddt\{IRP\}[t] / IRP[t]) < 1.0e-4} \\
\varphi_{S5} &= \texttt{abs(ddt\{TfR1\}[t] / TfR1[t]) < 1.0e-4}
\end{aligned} \tag{13}$$

(To make the reading easier, all formula dealing with the iron-replete steady state will begin by "φ_S", formula related to parameters will begin by "φ_P" and formula related to the behavior will begin by "φ_B".) To check that the value of each variable at the steady state is in the intervals shown in table 1, or deduced

in 4.2, we use the following formula:

$$\begin{aligned}
\varphi_{S6} &= \texttt{(3.5e-8 < Fe[t])} \\
\varphi_{S7} &= \texttt{(3.0e-9 < IRP[t]) and (IRP[t] < 1.07e-8)} \\
\varphi_{S8} &= \texttt{(1.0e-8 < TfR1[t]) and (TfR1[t] < 8.7e-8)} \\
\varphi_{S9} &= \texttt{(1.04e-13 < FPN1a[t]) and (FPN1a[t] < 1.0e-5)} \\
\varphi_{S10} &= \texttt{(1.0e-13 < Ft[t]) and (Ft[t] < 1.0e-5)}
\end{aligned} \tag{14}$$

As the maximal concentration of iron is 2×10^{-6} mol/L all the time, and not only at the steady state, we do not enforce this property here.

Then, when the iron input is switched off, and the iron level becomes too low, the ferritins release iron. This release is due to a lower ferritin production rate, which provokes a decrease of ferritin concentration. This can only be triggered by crossing the threshold $\theta_{IRP \to Ft}$. This agrees with the previous statement that the variable describing IRP activity is lower than $\theta_{IRP \to Ft}$ under iron-replete conditions. We verify that property with the following formula:

$$\varphi_{S11} = \texttt{IRP[t] < theta\_IRP\_Ft} \tag{15}$$

This increase of IRP activity can only be triggered by a decrease in iron concentration important enough to cross the threshold $\theta_{Fe \to IRP}$. This is in line with the already indicated inequality $Fe > \theta_{Fe \to IRP}$ under iron-replete conditions. The corresponding formula is:

$$\varphi_{S12} = \texttt{Fe[t] > theta\_Fe\_IRP} \tag{16}$$

Moreover, when the iron level becomes too low, the FPN1a concentration is expected to become lower. This, also, can only be triggered by a crossing by IRP of the threshold $\theta_{IRP \to FPN1a}$. That means that in the iron-replete steady state the FPN1a concentration is above this threshold, which is expressed by this formula:

$$\varphi_{S13} = \texttt{IRP[t] < theta\_IRP\_FPN1a} \tag{17}$$

Nevertheless , as explained in section 3.4 (resp. section 3.3), the regulation by IRP on FPN1a ($k_{IRP \to FPN1a}$) (resp. on Ft ($k_{IRP \to Ft}$)) cannot be higher that the basal production rate of FPN1a (k_{FPN1a_prod}) (resp. Ft (k_{Ft_prod})). The formula imposing that are:

$$\varphi_{P1} = \texttt{k\_IRP\_FPN1a <= k\_FPN1a\_prod} \tag{18}$$

and

$$\varphi_{P2} = \texttt{k\_IRP\_Ft <= k\_Ft\_prod} \tag{19}$$

The activation of the regulatory system leads to the conservation of the iron level. We express that by enforcing the existence of a plateau of this level after shutting the iron import off. We want this plateau to exist for at least ten hours. To avoid incorrect simulations for which the concentration of this plateau is zero, we set it at, at least, one tenth of the concentration in the iron-replete situation. The following property expresses that:

$$\begin{aligned}
\varphi_{B1} = \texttt{ev_[6*3600, inf] (alw_[0, 10*3600]} \\
\texttt{((}\varphi_{S1}\texttt{) and (Fe[t] > 0.01*Fe[4*3600])))}
\end{aligned} \tag{20}$$

When the iron stored in ferritin is exhausted, the iron concentration eventually decreases to zero. Ferritin disappearance precedes iron depletion which is not rescued by replenishment from any internal store, in contrast to the transient phase immediately following removal of iron input from transferrin (Figure 2 A. Otherwise, it would mean that the cell has stored iron but is not using it, which contradicts the conditions set in 3.1. This implies that the parameter describing the strength of the regulation by the IRP (i.e. $k_{IRP \to Ft}$) is slightly lower or equal to the production rate (i.e. k_{Ft_prod}). We input this constraint with the following formula:

$$\varphi_{P3} = \texttt{k\_Ft\_prod*0.95 <= k\_IRP\_Ft} \tag{21}$$

Next, in table 1, two properties are expressed: the first enforces that the iron concentration is never higher than 2×10^{-6} mol/L, and the second enforces that the inequality $k_{Fe\_cons} \geq k_{Fe\_export} \cdot FPN1a$ holds in iron-replete situation. The corresponding formula are:

$$\varphi_{B2} = \texttt{alw (Fe[t] < 2e-6)} \tag{22}$$

and

$$\varphi_{S14} = \texttt{k\_Fe\_cons > k\_Fe\_export*FPN1a[t]} \tag{23}$$

Finally, we have to define formula linking all the previous formula. For this purpose, we first define the formula φ_{Sall} which aggregates all formula related to the steady state. As we want to be sure that, before the iron input is switched off, the system reaches and stays at the steady state, we enforce that the properties related to the steady state hold at least for one hour before the sixth hour. This formula expresses that:

$$\varphi_{Sall} = \texttt{ev\_[0,6*3600] (alw\_[0,3600] (}\varphi_{S1}\texttt{ and (}\varphi_{S2}\texttt{ and (}\varphi_{S3}\texttt{ and (... and }\varphi_{S14}\texttt{))))} \tag{24}$$

We also define the formula φ_{BPall} enforcing that all formula related to parameters or behavior are satisfied:

$$\varphi_{BPall} = \varphi_{P1}\texttt{ and (}\varphi_{P2}\texttt{ and (}\varphi_{P3}\texttt{ and (}\varphi_{B1}\texttt{ and }\varphi_{B2}\texttt{)))} \tag{25}$$

And finally, the formula φ_{all}, which enforces that all properties are satisfied:

$$\varphi_{all} = \texttt{(}\varphi_{Sall}\texttt{) and (}\varphi_{BPall}\texttt{)} \tag{26}$$

It is noticeable that no information on TfR1 in the iron-depleted situation nor on the parameters acting on it appears in this analysis. This is because, as we totally cut the entry of iron into the cell, variations in the concentration of TfR1 do not change the amount of incoming iron.

4.4 A robust valid region

Having defined the formula which expresses the relevant properties, we search for a subspace where all parameter sets verify these properties, by first finding a valid instantiation of the parameters and then exploring a neighborhood of this instantiation. In section 4.2, we found an initial parameter set, $\mathscr{P}_0$, satisfying constraints on the data for the steady state. It turns out that the simulation computed with this parameter set, shown in Figure 2 A, also verifies φ_{all}. As the temporal formula describes the expected qualitative behavior, this simulation is representative of the behavior of all trajectories in the region that we are looking for. We look around this point (in parameter space) to find a region exhibiting the expected behavior. To ensure that the formula φ_{P2} and φ_{P3} are satisfied, we enforce that $k_{IRP \to Ft}$ is

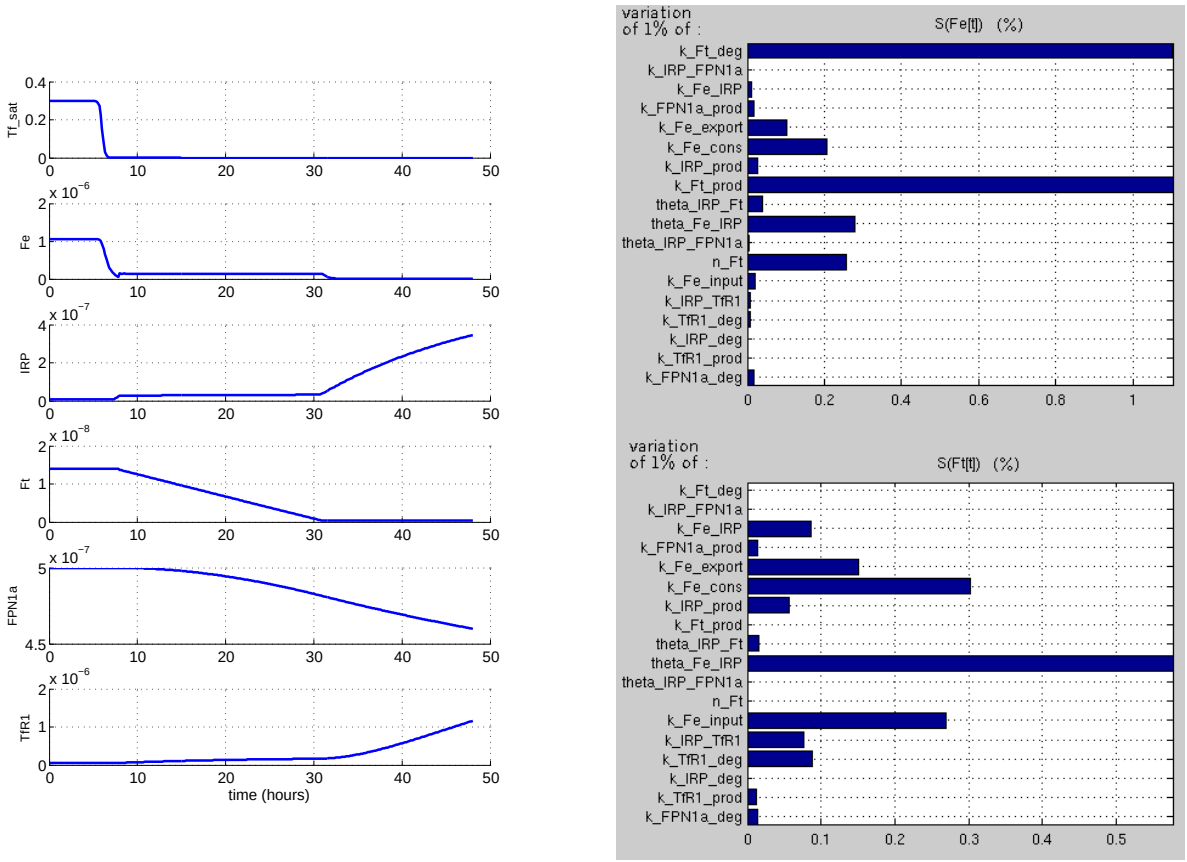

A) B)

Figure 2: A) Characteristic simulation of the expected qualitative behavior. It shows that the system switches to a new mode when iron is lacking. The parameter set used is $\mathscr{P}_0$. At time t=6 hours, Tf_{sat} is set to zero. The iron concentration consequently decreases, leading to an increase of IRP activity. This increase leads to a decrease in Ft concentration, keeping the iron level constant. This also leads to a decrease in FPN1a concentration and to an increase in TfR1 concentration. During this phase when iron is kept constant, the concentration of iron is close to the threshold $\theta_{Fe\to IRP}$ and IRP activity is close to the thresholds $\theta_{IRP\to FPN1a}$ and $\theta_{IRP\to Ft}$. Once Ft concentration is zero, the iron concentration tends also to zero.
B) Histogram showing the sensitivity of iron and ferritin concentration to variations of parameter value. These results are normalized: for example, a variation of 1% in k_{Fe_cons} value leads to a variation of 0.2% in Fe value. To avoid incorrect sensitivity due do an initial transient phase of large amplitude, we do not consider the first three hours when computing the sensitivity. Moreover, as the behavior of the cell (i.e. death) changes when iron is totally exhausted, we consider the sensitivity only between t=3 hours and t=20 hours.

computed equal to $0.97 \times k_{ft\_prod}$. Moreover, if the parameter k_{FPN1a_prod} is lower than $k_{IRP\to FPN1a}$, we switch them to force that the formula φ_{P1} is satisfied. So, the dimension of the search space is slightly reduced.

To guide the search, we compute the sensitivity of the system to parameters. We show in Figure 2 B the sensitivity of iron and ferritin concentration to a variation of parameters value. Sensitivity to ferro-

portin, transferrin receptor and IRP are also computed, but are not shown. We define the sensitivity to a parameter as the maximal sensitivity of the five variables of this parameter. This sensitivity is used in the following manner: if the system is very sensitive to a parameter, we will explore a close neighborhood of this parameter. On the opposite, if the system sensitivity to a parameter is low, we will explore a large neighborhood. Nevertheless, it has to be noted that the system can be very sensitive to a parameter, and that even with large variations on this parameter the qualitative property is still satisfied. This happens when the sensitivity which is detected affects an aspect of the trajectories which is not captured by the property of interest.

To verify that all simulations corresponding to a parameter subspace exhibit the expected behavior, we performed intensive trajectory computations. We randomly picked 10000 parameter sets within this subspace and checked the truth value of the formula φ_{all}. By expanding as much as possible the parameter interval, we found an hyper-rectangle centered on $\mathscr{P}_0$ such that all parameter sets in this region exhibit the expected behavior. Some parameters of $\mathscr{P}_0$ could change up to 70% of their initial value, with an average of 34% for all, while conserving the behavior of the system.

We observe that for the whole region of parameter space characterized in the iron-depleted situation, the FPN1a concentration remains at a rather high level, implying the considered cell keeps its ability to export iron despite shortage of the metal.

5 Conclusion

Two models of the core iron homeostasis system have been published previously. Omholt et al [22] aim at building a "unifying meta-model", that is a model which is not tied to a particular cell type. They include explicitly the two different Iron Regulatory Proteins, IRP1 and IRP2. Both proteins have the same mRNA targets, so they seem to be redundant, but they respond to the iron level in the cell through different molecular mechanisms. The model of Omholt et al [22] does not explicitly include ferritin nor ferroportin. In addition, all interactions in the network are switch-like (sigmoidal kinetics). A numerical value was assigned to all parameters except the sigmoid steepness, and the stability of the unique steady state was monitored as the sigmoid steepness is varied. The more recent paper of Chifman et al [5] is closer to our approach. This model considers the same five biological species, but the analytical expression of their differential system is different from ours. The major differences are for the IRP, ferritin and ferroportin equations (note that the graph shown in figure 1 of [5] does not follow the formal definition given here for an interaction graph). The mathematical analysis of the parametrized model of [5] is general in the sense that it does not rely on parameter instantiation. They showed that the model produces a single steady state, the stability of which was studied by performing simulations with sampled parameter values.

Here we have chosen an approach intermediate between Omholt et al [22] and Chifman et al [5]: a parametrized model has been built without imposing numerical values to the parameters. The available experimental data allowed us to apply inequality constraints between the parameters, together with behavioral constraints expressed in a temporal logic formalism. We could thus study not only steady states, but also dynamical responses to perturbations, as, for instance, the sharp decrease of iron input, starting from an iron-replete cell state. The region of parameter space for which the model exhibits the observed behavior has been characterized. It appeared that, in the iron-depleted situation, the FPN1a concentration remains at a rather high level, implying the considered cell kept its ability to export iron despite shortage of the metal. This is a significant outcome of modeling which justifies that another regulatory mechanism than that of the IRP may be needed under these conditions. This additional regulation may be provided

by FPN1a degradation by hepcidin.

We plan to extend the present model. For example the influence of iron on the inhibition of IRP activity involves the iron cluster biosynthesis pathway which will be introduced in the model. Also, the regulatory mechanisms of IRP could be described more precisely by integrating mRNA concentrations in the model. These extensions will be performed in a controlled and stepwise manner. The qualitative behavior will be compared with that of the core model presented here. This will give an insight into the robustness of the dynamical property of interest.

Acknowledgments

This work was supported by Microsoft Research through its PhD Scholarship Programme.
The authors thank the Région Rhône-Alpes for financial support within the Cible 2010 Program.

References

[1] P. Aisen (2004): *Transferrin receptor 1*. The International Journal of Biochemistry &; Cell Biology 36(11), pp. 2137–2143, doi:10.1016/j.biocel.2004.02.007.

[2] N. C. Andrews (2008): *Forging a field: the golden age of iron biology*. Blood 112(2), pp. 219–230, doi:10.1182/blood-2007-12-077388.

[3] P. Arosio & S. Levi (2010): *Cytosolic and mitochondrial ferritins in the regulation of cellular iron homeostasis and oxidative damage*. Biochim. Biophys. Acta 1800(8), pp. 783–792, doi:10.1016/j.bbagen.2010.02.005.

[4] O. S. Chen, K. P. Blemings, K. L. Schalinske & R. S. Eisenstein (1998): *Dietary iron intake rapidly influences iron regulatory proteins, ferritin subunits and mitochondrial aconitase in rat liver*. J. Nutr. 128(3), pp. 525–535.

[5] J. Chifman, A. Kniss, P. Neupane, I. Williams, B. Leung, Z. Deng, P. Mendes, V. Hower, F. M. Torti, S. A. Akman, S. V. Torti & R. Laubenbacher (2012): *The core control system of intracellular iron homeostasis: a mathematical model*. J. Theor. Biol. 300, pp. 91–99, doi:10.1016/j.jtbi.2012.01.024.

[6] L. Cianetti, P. Segnalini, A. Calzolari, O. Morsilli, F. Felicetti, C. Ramoni, M. Gabbianelli, U. Testa & N. M. Sposi (2005): *Expression of alternative transcripts of ferroportin-1 during human erythroid differentiation*. Haematologica 90(12), pp. 1595–1606.

[7] I. De Domenico, D. McVey Ward & J. Kaplan (2008): *Regulation of iron acquisition and storage: consequences for iron-linked disorders*. Nat. Rev. Mol. Cell Biol. 9(1), pp. 72–81, doi:10.1038/nrm2295.

[8] A. Donzé (2010): *Breach, A Toolbox for Verification and Parameter Synthesis of Hybrid Systems*. In: CAV, pp. 167–170, doi:10.1007/978-3-642-14295-6_17.

[9] A. Donzé, É. Fanchon, L. M. Gattepaille, O. Maler & P. Tracqui (2011): *Robustness Analysis and Behavior Discrimination in Enzymatic Reaction Networks*. PLoS ONE 6(9), p. e24246, doi:10.1371/journal.pone.0024246.

[10] A. Donzé & O. Maler (2010): *Robust Satisfaction of Temporal Logic over Real-Valued Signals*. In: FORMATS, pp. 92–106. Available at `http://dx.doi.org/10.1007/978-3-642-15297-9_9`.

[11] C. Dycke, P. Charbonnier, K. Pantopoulos & J. M. Moulis (2008): *A role for lysosomes in the turnover of human iron regulatory protein 2*. Int. J. Biochem. Cell Biol. 40(12), pp. 2826–2832, doi:10.1016/j.biocel.2008.05.015.

[12] S. Epsztejn, O. Kakhlon, H. Glickstein, W. Breuer & I. Cabantchik (1997): *Fluorescence analysis of the labile iron pool of mammalian cells*. Anal. Biochem. 248(1), pp. 31–40.

[13] R. Erlitzki, J. C. Long & E. C. Theil (2002): *Multiple, conserved iron-responsive elements in the 3'-untranslated region of transferrin receptor mRNA enhance binding of iron regulatory protein 2*. J. Biol. Chem. 277(45), pp. 42579–42587, doi:10.1074/jbc.M207918200.

[14] . Funahashi, M. Morohashi, H. Kitano & N. Tanimura (2003): *CellDesigner: a process diagram editor for gene-regulatory and biochemical networks*. BIOSILICO 1(5), pp. 159–162, doi:10.1016/S1478-5382(03)02370-9.

[15] D. Galaris & K. Pantopoulos (2008): *Oxidative stress and iron homeostasis: mechanistic and health aspects*. Crit Rev Clin Lab Sci 45(1), pp. 1–23, doi:10.1080/10408360701713104.

[16] L. Granvilliers & F. Benhamou (2006): *Algorithm 852: RealPaver: an interval solver using constraint satisfaction techniques*. ACM Transactions on Mathematical Software 32(1), pp. 138–156, doi:10.1145/1132973.1132980.

[17] R. C. Hunt & L. Marshall-Carlson (1986): *Internalization and recycling of transferrin and its receptor. Effect of trifluoperazine on recycling in human erythroleukemic cells*. J. Biol. Chem. 261(8), pp. 3681–3686.

[18] M. D. Knutson, M. Oukka, L. M. Koss, F. Aydemir & M. Wessling-Resnick (2005): *Iron release from macrophages after erythrophagocytosis is up-regulated by ferroportin 1 overexpression and down-regulated by hepcidin*. Proc. Natl. Acad. Sci. U.S.A. 102(5), pp. 1324–1328, doi:10.1073/pnas.0409409102.

[19] Maxima (2011): *Maxima, a Computer Algebra System. Version 5.24.0*. Available at `http://maxima.sourceforge.net/`.

[20] R. Mayr, A. R. Janecke, . Schranz, W. J.H. Griffiths, W. Vogel, A. Pietrangelo & H. Zoller (2010): *Ferroportin disease: A systematic meta-analysis of clinical and molecular findings*. Journal of Hepatology 53(5), pp. 941–949, doi:10.1016/j.jhep.2010.05.016.

[21] R. Moirand, A. M. Mortaji, O. Loréal, F. Paillard, P. Brissot & Y. Deugnier (1997): *A new syndrome of liver iron overload with normal transferrin saturation*. The Lancet 349(9045), pp. 95–97, doi:10.1016/S0140-6736(96)06034-5.

[22] S. W. Omholt, X. Kefang, Ø. Andersen & E. Plahte (1998): *Description and Analysis of Switchlike Regulatory Networks Exemplified by a Model of Cellular Iron Homeostasis*. Journal of Theoretical Biology 195(3), pp. 339–350, doi:10.1006/jtbi.1998.0800.

[23] M. Shvartsman, E. Fibach & Z. I. Cabantchik (2010): *Transferrin-iron routing to the cytosol and mitochondria as studied by live and real-time fluorescence*. Biochem. J. 429(1), pp. 185–193, doi:10.1042/BJ20100213.

[24] J. Wang & K. Pantopoulos (2011): *Regulation of cellular iron metabolism*. Biochem. J. 434(3), pp. 365–381, doi:10.1042/BJ20101825.

[25] A. M. Weissman, R. D. Klausner, K. Rao & J. B. Harford (1986): *Exposure of K562 cells to anti-receptor monoclonal antibody OKT9 results in rapid redistribution and enhanced degradation of the transferrin receptor*. The Journal of Cell Biology 102(3), pp. 951–958, doi:10.1083/jcb.102.3.951.